Available online at www.sciencedirect.com
SCIENCE DIRECT®
ELSEVIER
Earth and Planetary Science Letters 219 (2004) 221–238
EPSL
www.elsevier.com/locate/epsl

The Quaternary impact record from the Pampas, Argentina

Peter H. Schultz [a,*], Marcelo Zárate [b], Bill Hames [c], Christian Koeberl [d], Theodore Bunch [e], Dieter Storzer [f], Paul Renne [g], James Wittke [e]

[a] *Department of Geological Sciences, Brown University, Providence, RI 02912-1846, USA*
[b] *Facultad de Ciencias Exactas y Naturales, Universidad Nacional de La Pampa, Av. Uruguay 151, 6300 Santa Rosa, La Pampa, Argentina*
[c] *210 Petrie Hall Department of Geology, Auburn University, Auburn, AL 36830, USA*
[d] *Department of Geological Sciences (Geochemistry), University of Vienna, Althanstrasse 14, A-1090 Vienna, Austria*
[e] *Bilby Research Center, Northern Arizona Research Center, Department of Geology, Flagstaff, AZ 86011, USA*
[f] *Muséum d'histoire naturelle, Laboratoire de Minéralogie, 61 rue Buffon, 75005 Paris, France*
[g] *Berkeley Geochronology Center, 2455 Ridge Road, Berkeley, CA 94709, USA*

Received 25 June 2003; received in revised form 18 December 2003; accepted 22 December 2003

Abstract

Loess-like deposits cover much of central Argentina and preserve a rich record of impacts since the late Miocene. The present contribution focuses on two localities containing Quaternary impact glasses: along the coastal sequences near Centinela del Mar (CdM) and from near Rio Cuarto (RC). These highly vesicular glasses contain clear evidence for an impact origin including temperatures sufficient to melt most mineral constituents (1700°C) and to leave unique quench products such as β-cristobolite. The CdM glasses occur within a relatively narrow horizon just below a marine transgression expressed by a series of coastal paleo-dunes and systematic changes in the underlying sediments. High-resolution $^{40}Ar/^{39}Ar$ dating methods yielded an age of 445 ± 21 ka (2σ). Glasses were also recovered from scattered occurrences lower in the section but were dated to 230 ± 40 ka. This inconsistency between stratigraphic and radiometric age is most likely related to a nearby outcrop of glass that had been exposed and locally re-deposited in coastal lagoons during the last marine transgression at 125 ka. Sediments containing the original impact glass layer are now missing due to an unconformity, perhaps related to subsequent marine transgressions after the impact (410 ka and 340 ka) and hiatuses in deposition. Two different types of impact glasses from RC yield two distinct dates. High-resolution $^{40}Ar/^{39}Ar$ dating of fresher-appearing glasses (well-preserved tachylitic sheen) indicates an age of 6 ± 2 ka (2σ). Independent fission track analyses yielded a similar age of 2.3 ± 1.6 ka (2σ). More weathered glasses, however, gave significantly older ages of 114 ± 26 ka (2σ). Consequently, materials from two separate Quaternary impacts have been recovered at Rio Cuarto. The younger glasses are consistent with previously reported carbon dates for materials on the floor of one of the large elongate structures. The depths of excavation for the RC and CdM impacts are very different. While the RC glasses are largely derived from near-surface materials, the CdM glasses from the upper level contain added components consistent with Miocene marine evaporites at a depth of about 400–500 m (e.g., high CaO and P_2O_5). The CdM glasses also incorporated older loess-like sediments from depth based on the geochemistry. Several ratios of key trace and rare earth elements of sediments of different ages from the Miocene to the Holocene

* Corresponding author.
E-mail address: peter_schultz@brown.edu (P.H. Schultz).

0012-821X/04/$ – see front matter
doi:10.1016/S0012-821X(04)00010-X

indicate a systematic compositional change through time. Such changes calibrate the observed differences in glass composition from their host sediments and further indicate incorporation of materials from depth. Consequently, the Argentine loess-like sediments preserve evidence for at least four separate Quaternary impacts. Based on foreign components in the glasses, the CdM impact very likely produced a crater (now buried or eroded) once as large as 6 km in diameter. The younger RC glasses, however, are consistent with shallower excavation consistent with an oblique impact.

Keywords: impact glass; Argentina; escoria; pampasites; loess; tektites

1. Introduction

The Quaternary impact-cratering record in North America and Europe is poorly preserved due to repeated glaciations and their consequences. Crater structures have been stripped to their roots, eroded away, or buried by sediments. While certain regions (such as the Williston basin including portions of Wyoming, Montana, North Dakota) retain numerous Cretaceous craters stacked within sediments in the same area [1], they are buried by thick sequences and are revealed only by seismology and drilling. And the continuous pelagic record in the Italian Umbria–Marche Sequence, spanning 230 Myr, contains only a few global/regional impact layers [2]. There are even fewer locations that provide a relatively continuous record of on-land collisions accessible for field studies.

The vast loess and loess-like deposits comprising the Pampas materials of Argentina, however, represent a unique loess-like depositional sequence extending back to the late Miocene (see [3] for a review). Within these deposits, five impact glass horizons have been reported (see Fig. 1 and Table 1) and extend from the Holocene into the Miocene: near Rio Cuarto [4–6]; within the cliffs near Mar del Plata [7]; near Necochea [8]; near Bahía Blanca [9]; and near Chasicó [8,10]. The rich impact record may seem anomalous. But the large number of occurrences in the Late Cenozoic Pampean sedimentary record represents the efficiency of generating glass from particulate targets, their preservation potential once captured, and the absence of other fragmental debris that might mask easy identification of such materials. Based on the terrestrial cratering record [11], Pampean sediments covering one million square kilometers could contain almost 20 craters larger than 1.0 km in diameter over the last 10 Myr, seven craters over the last 2.5 Myr and perhaps three in the last 1 Myr.

Here we present the first detailed accounting of the Pleistocene impact glasses near Necochea at a locality called Centinela del Mar (CdM). These glasses are compared with nearby Pliocene glasses of Chapadmalal near Mar del Plata (MdP) and Holocene impact materials from Rio Cuarto (RC). As described below, new radiometric and fission track ages for the RC impact now establish this as a historical impact. The CdM glasses are important for several reasons. First, they provide a record of products and processes resulting from a large impact into thick eolian sedimentary target. Second, the glasses appear to have incorporated marine sequences at depth or offshore. Third, the locality contains abundant fossils with-

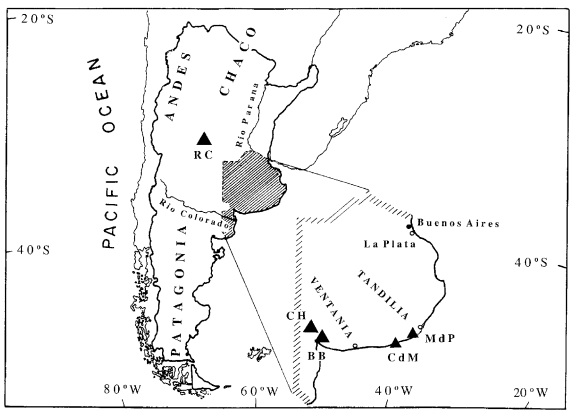

Fig. 1. Location of study area at Centinela del Mar (CdM) as well as Chapadmalal near Mar del Plata (MdP) to the northeast along the coast and Rio Cuarto (RC) inland. Also shown are exposures of impact glasses near Chasicó (CH) and Bahía Blanca (BB), which are noted in Table 1.

Table 1
Summary of localities, ages, and references for impact materials discussed here

Location	Stratigraphic age	Glass age[a]	Technique[b]	Reference
Rio Cuarto (RC)				
A. Fresh	Holocene	4–10 ka	gc	[4,5]
		2.3 ± 01.6 ka	ft	This study
		6 ± 2 ka	r	This study
B. Old	Pleistocene	570 ± 100 ka	r	[6]
		114 ± 26 ka	r	This study
Centinela del Mar (CdM)	Pleistocene			
A. LCdM		230 ± 30 ka	r	This study
B. UCdM		445 ± 21 ka	r	This study
Mar del Plata (MdP)	Pliocene	3.27 ± 0.08 Ma	r	[7]
Bahía Blanca	Late Miocene	5.33 ± 0.05 Ma	r	[9]
Chasico	Late Miocene	9.23 ± 0.09 Ma	r	[8][c]

[a] Uncertainty given as 2σ.
[b] gc = geologic context (stratigraphy, preservation state); ft = fission track; r = radiometric $^{40}Ar/^{39}Ar$.
[c] Represents a revision from the age cited in [8].

out a detailed stratigraphic context and independent ages that now can be constrained by the dated glasses. And fourth, a poorly time-constrained record of a Pleistocene marine transgression (ca. 125 ka) occurs within the deposits [12].

2. Geologic setting

In contrast with the high ocean cliffs of loessoid deposits near Mar del Plata, the Argentine coast between Miramar and Necochea forms low-relief coastal beaches with low cliff sections and dunes. One exception is near Centinela del Mar, where 10 m cliffs extend for about 2.5 km and contain important Late Cenozoic outcrops. Numerous vesicular, slag-like glasses (locally called 'escorias') outcrop in two associated horizons near the top of this section (UCdM) and closely resemble previously reported glasses from those from RC and near MdP. Widely scattered escoria fragments rarely occur at other levels within the sediments and typically represent reworked distal materials from other events, such as the Pliocene impact near Mar del Plata. But another less well-defined layer of widely dispersed glasses outcrops at certain locations about 3 m below the UCdM. These glasses (LCdM) typically exhibit evidence for transport (rounding, smaller fragments).

The UCdM glasses occur within a paleosol sequence developed on sandy silt facies (see Fig. 2). They were deposited within a coastal lagoon environment now covered by a paleo-dune littoral barrier showing megascale cross stratification [12]. The coastal lagoon facies consists of sandy silts that display pedogenic features giving way to a paleosol sequence. The greatest concentration, however, occurs within a 5–10 cm thick layer, only about 15 cm from the top of the paleosol (A horizon).

Over 100 UCdM and 10 LCdM glass samples have been recovered from the CdM section. The largest UCdM masses approach 10 cm across and typically occur at a specific horizon as clusters in association with red brick-like masses (tierra cocidas). Some of these glasses appear to have been emplaced while still molten, as indicated by textured casts on one side and cooling surfaces on the other. Many are largely intact and retain fragile structures. Consequently, there is little evidence for high-energy or continuous fluvial transport over large distances. A secondary concentration occurs just below (20–50 cm), but this is composed of small (<2 cm), broken, and dispersed fragments consistent with later bioturbation from the primary concentration of UCdM glasses. Broken fragments are also widely scattered within the overlying paleo-dunes as a result of later reworking.

The CdM glasses differ from both the younger

Fig. 2. Cliff sequence near Centinela del Mar where impact glasses outcrop within a narrow horizon (arrow).

RC and older MdP glasses in detail (Fig. 3). First, most CdM glasses exhibit higher fractions (80–90 vol%) of clear glass, whereas both the RC and MdP glasses exhibit a wider range in clear glass (10–90 vol%). Second, thin sections reveal both well-preserved elongate to rounded vesicles and a few irregular vesicles suggestive of collapse. And third, the glass surfaces commonly exhibit smooth buds and extensions. Thin sections reveal flow through narrow openings in the surface and 'blooming' into buds. This pattern indicates breaking of a cooled crust with extrusions before complete quenching. There is evidence for dynamic emplacement with folds and zones of less melted material attached, similar to glasses from other Argentine localities.

3. Impact glasses

3.1. Petrology

Different types of CdM glasses (eight samples) were thin sectioned for petrologic and electron microprobe analyses. Samples were selected on the basis of geographic location, position in section, and appearance. This strategy allows assessing possible diversity due to distance from the crater (location still unknown), reworking (position in section), and temperature history (appearance). Regardless of physical appearance (e.g., vesicularity and size) the UCdM glasses are all remarkably similar. Most contain unmelted phases comprising less than 10 vol%. One heterogeneous sample contained two parts: one with 10 vol%, the other <40 vol% unmelted. Vesiculation ranges from 30 vol% to more than 60 vol%, but typically is 40–50 vol%. The dominant unmelted phases are rounded quartz grains with feldspar (K-feldspars and plagioclase with K-feldspars predominate over plagioclase 3:1) generally a minor component (excepting two samples). Quench crystals are generally rare (but see below), again excepting the one heterogeneous sample. As illustrated in Fig. 4, flow structure (schlieren) and shrinkage cracks are common.

Shock signatures in the Argentine glasses are primarily limited to evidence of extremely high transient temperatures and rapid quenching. Highly porous (and wet) targets subjected to intense shock typically do not exhibit classic shock indicators (e.g., planar deformation features) as discussed elsewhere (e.g., [5,7]). The impactites here contain diaplectic glass (quartz, feldspars), baddeleyite, distinctive mineral mixtures, and reaction rims indicative of intense heating and rapid cooling. The geologic context, evidence for dynamic flow, and size of the glasses all indicate an origin by impact. Although these glasses might be classified as 'impact melt breccias' containing a variety of source materials, such a term departs from the classic definition involving fractured components of the source rock compressed together and mixed with melt components. In this case, the unmelted components are individual mineral grains that may have been entrained dur-

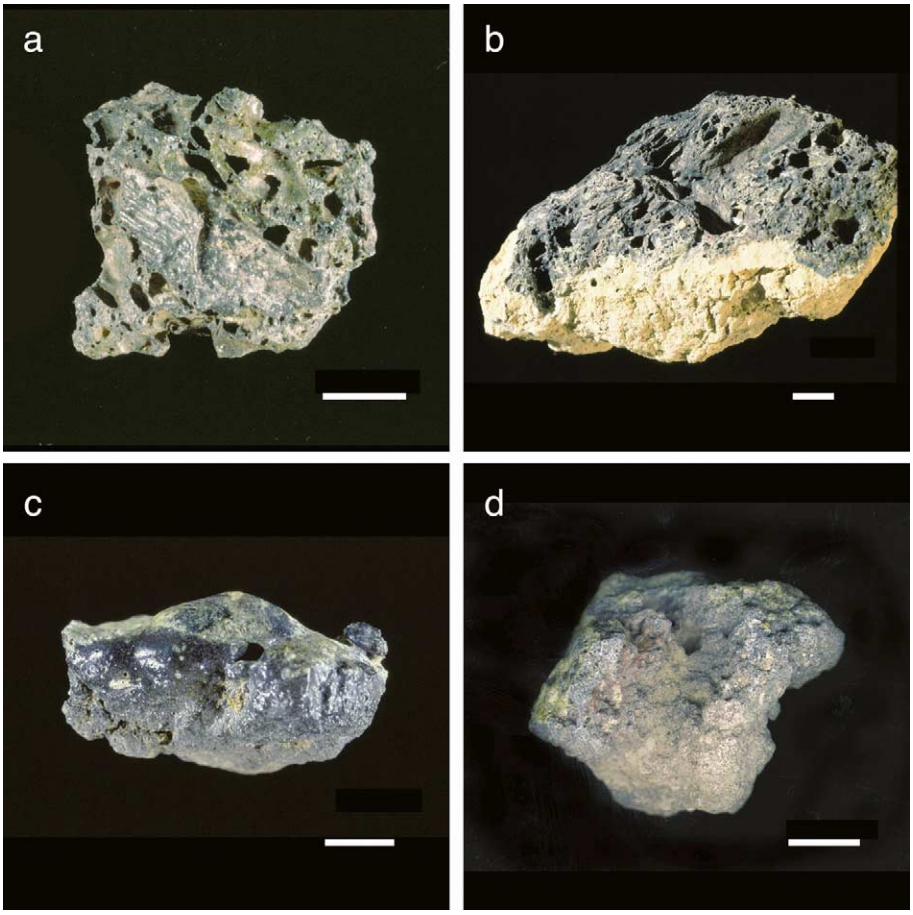

Fig. 3. Typical impact glass recovered from different localities discussed. Pleistocene glasses from CdM exhibit budding and other fragile textures still preserved (a). This contrasts with more weathered Pliocene glasses from MdP (b). The Quaternary RC glasses exhibit both very fresh-appearing glass (c) and more weathered glass (d). Scale bars represent 1 cm in a, c, and d but 2 cm in b.

ing ejection or dynamic emplacement while still semi-molten. Consequently, we are suggesting a new term, 'pampasites', to refer to the distinctive Argentine impact glasses created by melting of porous loess substrates.

Temperature can be inferred from the nearly complete melting of all constituents (including ~0.1 mm-sized quartz grains) to only the partial melting of mineral grains smaller than 40 μm. Large, remnant quartz in partially melted samples shows rounded grain margins and embayments. Melting of quartz grains in completely melted samples produced distinctive schlieren (Fig. 4) having contrasting refractive indices over distances of tens of micrometers, a product characteristic of intense heating and rapid quenching (e.g., [5]).

Temperatures were sufficiently high to completely melt many precursor materials and promote viscous flow with rapid out-gassing (vesicles). Temperatures above 1700°C are indicated based on nearly complete thermal digestion of all mineral constituents including quartz (Fig. 4). Qualitative cooling rates are highly variable among and within samples. For example, the highest cooling rates are completely melted samples and are devoid of quench products. Samples of slower cooling rates may contain isolated clusters of isotropic β-cristobalite, the high-temperature form of cristobolite, set in silica glass (Fig.

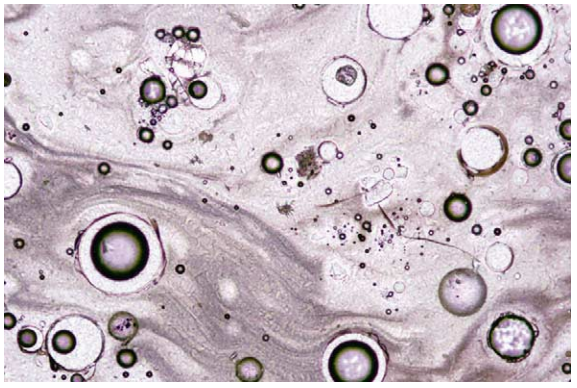

Fig. 4. Thin sections illustrating evidence for nearly complete melting of almost all constituents, including quartz. Rapid cooling is indicated by distinctive schlieren, partially melted clasts, and viscous flow.

5a). Identification of the β form is based on isotropic and octahedral crystal form characteristics that are unique to β-quartz. More specifically, β-quartz is hexagonal (not isotropic) and is invariably twinned; β-cristobalite is isometric (hence the octahedral outlines), isotropic, and untwinned. Crystals range from anhedral to octahedral outlines. β-Cristobalite is stable from 1470 to 1720°C, but typically inverts to the low-temperature α form at 268°C [13]. Only in rare occurrences can very rapid cooling rates allow β-cristobalite to exist in the metastable form at room temperatures, e.g., in blast furnace silica bricks and from high-temperature gas deposition in volcanically formed vesicles. Alternatively, the inversion from unstable β- to stable α-cristobalite can be arrested by encapsulation in glass [14]. Regardless, β-cristobolite rarely occurs naturally except in impact glasses, e.g., the Libyan Desert glass. Rapid cooling in the UCdM samples is also implied by the occurrence of acicular, bladed, and 'hopper' quench crystals of pyroxene, wollastonite, and melilite, some in association with tridymite (Fig. 5b,c). The high temperature, rapid quenching, and relatively restricted occurrence in a specific horizon all indicate an impact origin for these glasses.

3.2. CdM radiometric glass ages

Both high-resolution $^{40}Ar/^{39}Ar$ dating and fission track dating allow dating with sufficient accuracy to distinguish clearly between the CdM and RC Quaternary events. Glass samples were crushed and clear glass fractions (typically less than 400 μm) were hand-picked under magnification. A second and independent screening then eliminated remaining shards containing any xenocrysts and phenocrysts, evidence of alteration, and highly frothy components (trapped atmospheric gases). This process ensured that the ages measured would represent the closest possible approximation to the timing of glass formation by minimizing the potential effects of extraneous argon from 'undigested' constituent loess minerals, vesicles, or the effects of alteration. Earlier studies (e.g., [7]) discussed the bias and imprecision that can be introduced to analyses of escoria due to xenocrysts, alteration, and trapped atmospheric gases. Multiple samples were sampled and analyzed from outcrops at different localities.

Age determinations using $^{40}Ar/^{39}Ar$ were made at the Berkeley Geochronology Center with CO_2 laser incremental-heating extraction techniques as previously described [15]. Fish Canyon sanidine (28.02 Ma [16]) was used as a neutron fluence monitor during Cd-shielded irradiation in the Oregon TRIGA reactor. All ages are quoted at the 95% confidence level (excluding systematic errors due to decay constants and age of the standard). Interference corrections were based on data reported in [16]. Two UCdM samples yielded consistent $^{40}Ar/^{39}Ar$ ages as shown in Fig. 6A. Duplicate incremental heating analyses for glass from one UCdM escoria resulted in plateau ages of 460 ± 30 and 430 ± 30 ka. Averaging the results of these samples yields an age of 445 ± 21 ka for the glasses of UCdM.

Similar analyses for two runs of an LCdM glass fragment yielded consistent ages of 210 ± 40 ka and 230 ± 40 ka. The latter sample yielded a higher radiogenic yield and is considered more reliable. Hence there appears to be a paradox: the glasses lower in the column (LCdM) are younger than the glasses at the top of the section. This paradox most likely means that the upper glasses (UCdM) do not represent a primary deposit. Soon after the 445 ka UCdM glasses were depos-

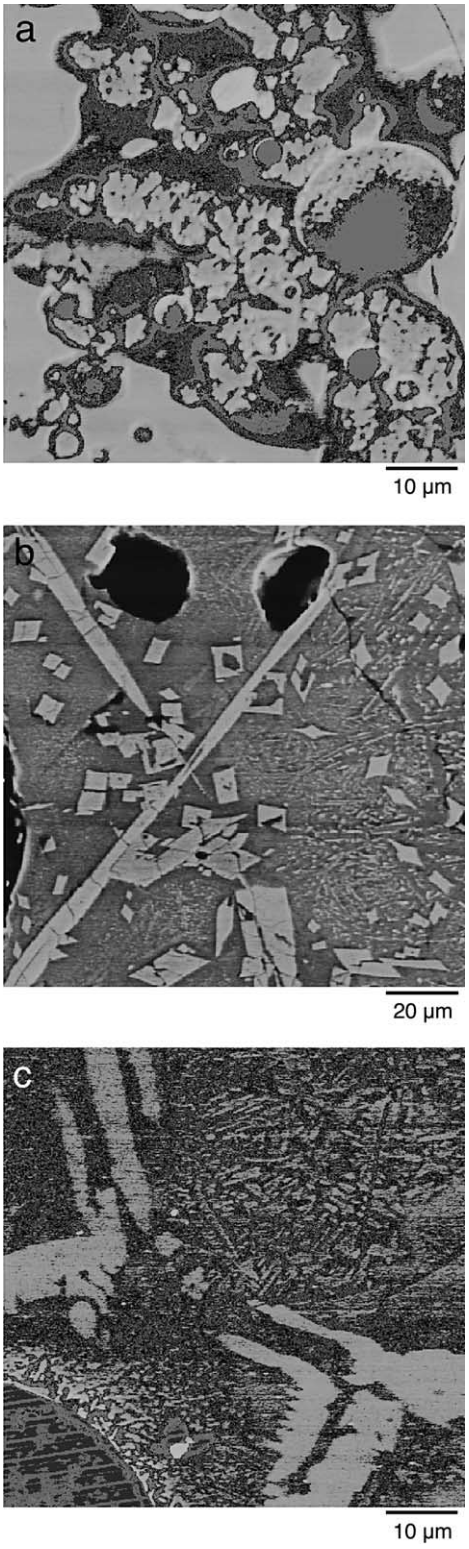

Fig. 5. SEM-BSE images of selected minerals in the CdM glasses. Panel a is an SEM-BSE image of β-cristobalite aggregates set in silica glass (dark), which is surrounded by melt glasses (light). Small to large round objects are vesicles. Panel b shows augitic pyroxene quench crystallites set in melt glasses. Panel c illustrates wollastonite (lightest) and melilite quench crystallites in melt glasses.
←

ited, a major marine transgression (410 ka) most likely removed the primary glass-bearing layer at the present locality, consistent with unconformities in the section. Preserved sections inland were then re-exposed and re-deposited in shallow depressions behind coastal barrier dunes during the last major transgression about 120 ka [12].

3.3. Rio Cuarto glass ages

Radiometric dating procedures followed the same approach for the CdM glasses and yielded much younger ages (Fig. 6B). There are two different types of decimeter-size glasses found at Rio Cuarto: very fresh-appearing folded glasses with a tachylitic sheen on the surface (Fig. 3c) and older-appearing (weathered) broken vesicular masses (Fig. 3d). The more weathered samples are typically found as surface lags within the larger elongate structures (see [4,5]). The fresh-appearing glasses were recovered both in section and as surface lag material as far as 150 km to the south-southwest. In earlier studies, it was assumed that the weathered glasses simply reflected more prolonged exposure within ephemeral lakes, which commonly form in depressions in the vicinity of Rio Cuarto. Data obtained for the present study, however, reveal two different ages for the two types of glasses (Fig. 6B). An escoria sample exhibiting the fresh tachylitic sheen yielded an isochron age of 6 ± 2 ka with an 'initial' $^{40}Ar/^{39}Ar$ value of 295.2 ± 0.9, consistent with entrapment of modern atmospheric argon in vesicles of this escoria (a similar, though less precise, plateau age of 3 ± 17 ka is also defined by data for this sample).

Results for two samples of the older-appearing escoria from Rio Cuarto, however, indicated a different age. A first sample yielded plateau and isochron ages of 130 ± 60 ka and 110 ± 30 ka, re-

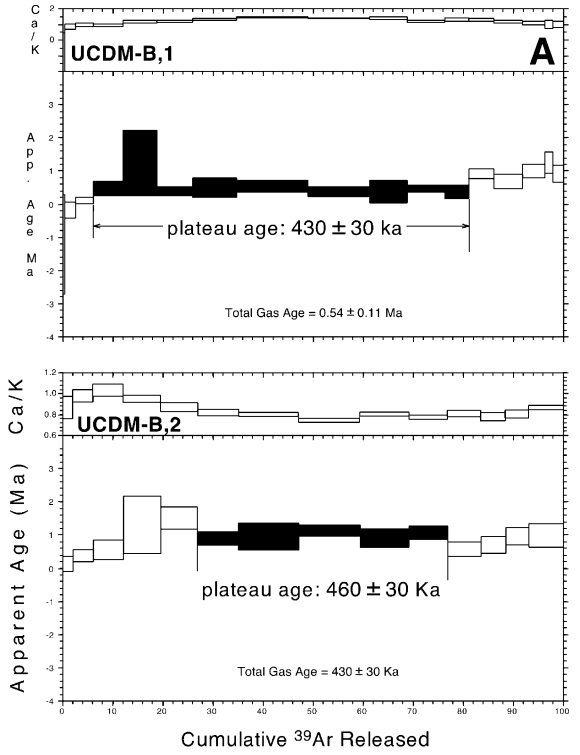

Fig. 6. (A) $^{40}Ar/^{39}Ar$ incremental heating spectra for two different splits of a single escoria sample, collected at the Centinela del Mar locality. The plateau and isochron age results for the samples are the same within uncertainty, and the samples appear characterized by a single component of radiogenic argon and trapped extraneous argon of atmospheric composition. (B) $^{40}Ar/^{39}Ar$ incremental heating release spectra for three samples collected in the vicinity of Rio Cuarto. The isochron age results for each sample are considered to be the most representative of the timing of escoria formation, as discussed in the text.

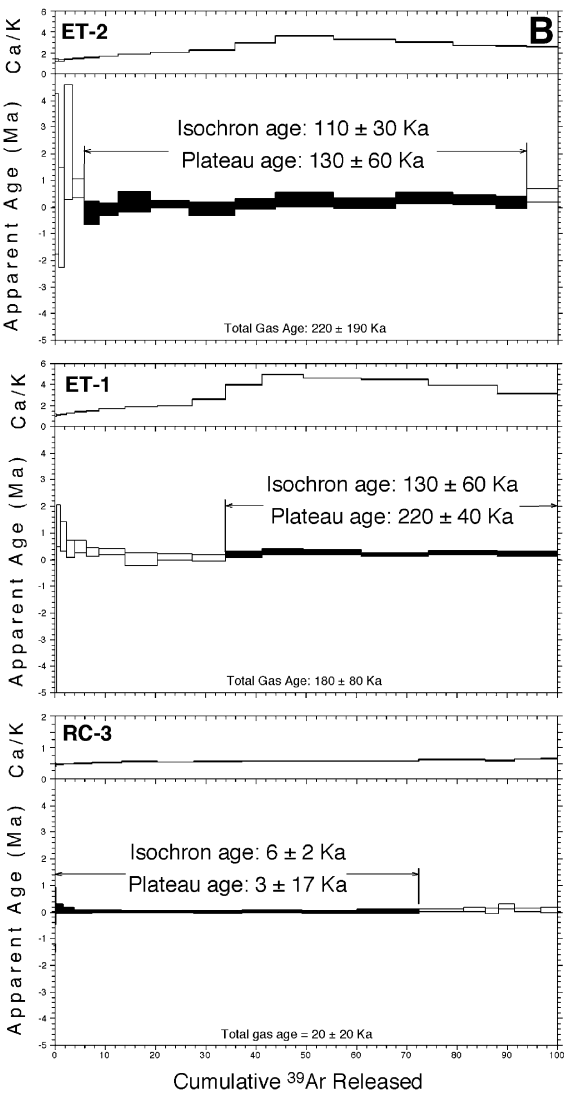

Fig. 6 (*Continued*).

spectively. The $^{40}Ar/^{39}Ar$ ratio of extraneous argon as suggested by the isochron treatment is indistinguishable from the modern atmosphere (296.2 ± 0.9), and the high relative uncertainty in the age determination is due to the low concentration of radiogenic argon and high proportion of trapped atmospheric argon. A second sample of the older-appearing escoria yielded an isochron age of 130 ± 60 ka, but with a slightly higher initial $^{40}Ar/^{39}Ar$ ratio of 298 ± 2 suggestive of a component of unsupported 'excess' ^{40}Ar (and resulting plateau age of 220 ± 40 ka). Our preferred interpretation for the older RC glasses is that they formed at 114 ± 26 ka, a result obtained as an average of the two isochron ages (weighted by their associated uncertainties).

Fission track analyses were also performed on two cm-sized splash-form impact glasses collected from the 'Eastern Twin' crater of the Rio Cuarto field noted in [2,5]. Fission track dating has been successfully applied during the last 30 years to tektites and impact glasses [17]. Seventeen disks (saw cuts about 0.8 mm thick) of these glasses were distributed among six sections, mounted in

epoxy, and polished. The glass disks consisted of a homogeneous core (devoid of any background of microlites or small bubbles which after etching might be mistaken for fission tracks) surrounded by a rim of vesicle-rich glass and trapped quartz crystals. The fossil fission tracks were developed by etching the six polished sections in an aqueous acid solution (2 vol. 40% HF+1 vol. 96% H_2SO_4+1 vol. 65% HNO_3+6 vol. H_2O). Fission tracks were then counted in reflected light under an optical microscope (ocular: 10×; objective: 50×) and their respective sizes (major axes) were determined under high magnification (ocular: 10×; objective: 160×).

Two of the six glass mounts were covered with KAPTON as an external fission track detector. They were then irradiated with a time-integrated thermal neutron flux of 1.13×10^{15} n/cm^2, together with a 14.87 ± 0.36 Ma old Moldavite age standard [18] and NBS reference glass: SRM 613. The irradiation was performed in the most thermalized position (channel P1) of the reactor Orphée at Saclay (France). The induced fission tracks, recorded on the external track detector KAPTON, were then revealed in an aqueous solution of 14% NaClO+12% NaCl, at 100°C, for 8 min. These induced fission tracks match the distribution of uranium in the glass phase and, therefore, can be used for uranium mapping. The two glass mounts, on the other hand, were re-polished, re-etched, and the induced fission tracks counted following the very same criteria as used formerly for the processing of the fossil fission tracks. For details on the technique and analytical data treatment, see [17–19].

Results of the fission track analyses are given in Table 2. The apparent mean fission track age of the Rio Cuarto impact glass, averaged over five glass mounts, and based on nine fossil fission tracks, converges to 2.3 ± 1.6 ka (2σ). The analytical uncertainty of the age value is the standard deviation as calculated from the quantities of fission tracks counted and the uncertainty for the integrated neutron fluence. Uranium is rather homogeneously distributed among the glass disks and converges to a mean content of 2.97 ± 0.16 ppm U. The nine fossil fission tracks were counted over a total area of 360 mm^2. Due to the high quality of the impact glass it is unlikely that any tracks were missed. On the other hand, lowering of the fission track age due to track fading can also be excluded. The mean size of the induced fission tracks is 6.64 ± 2.15 μm (305 tracks), of the nine fossil tracks 7.88 ± 0.59 μm. Although the number of size determinations for fossil tracks is low, the fact that the fossil tracks are not smaller than the induced tracks is an indication that the fission track age cannot be significantly lowered due to thermal effects.

Consequently, both radiometric and fission track dates for the fresher-appearing glasses yielded similar ages with comparable levels of relative precision. The younger fission track age of 2.3 ± 1.6 ka (2σ) is similar to the radiometric age of 6 ± 2 ka (2σ). The important conclusion to be drawn is that these two independent approaches on different fresh-appearing RC glass samples yielded comparably young ages consistent with previous conclusions based on stratigraphy and preservation state [4,5]. Moreover, an older glass component is also exposed in the structure, consistent with their more weathered appearance.

3.4. Composition

The different ages for RC and CdM glasses clearly establish that they represent different events. Differences in composition not only rein-

Table 2
Fission track analytical results

	Number of tracks	Scanned surface area (mm^2)	Track density (N/cm^2)	Age (ka) ($\pm2\sigma$)
Fossil tracks[a]	9	359.95	2.50 ± 0.83	2.3 ± 1.6
Induced tracks[b]	3978	6.406	$(6.21\pm0.31)\times10^4$	

[a] Constants used: $s_f=580.2\times10^{-24}$ cm^2; $I=7.253\times10^{-3}$; $l_f=8.46\times10^{-17}$/yr.
[b] Integrated thermal neutron fluence: $(1.13\pm0.11)\times10^{15}$ n/cm^2.

force this conclusion but also reveal contrasting source regions and excavation depths. Major element composition of the interstitial glasses were determined from electron microprobe analyses, whereas X-ray fluorescence (XRF) spectrometry and instrumental neutron activation analysis provided data for the bulk target materials and bulk impact glasses.

Tables 3 and 4 allow comparison of the major element contents of the RC, UCdM, and MdP glasses (bulk and just the clear glass components) as further illustrated in Fig. 7. A much larger suite of dated samples will be necessary to identify the unique characteristics of the two distinct impact glasses dated from RC simply on the basis of chemical composition alone. The RC samples generally match the near-surface loess composition [5,20]. The UCdM impact glasses, however, show very little intra- and inter-sample variation but their average bulk composition does not match that of sampled Pleistocene sediments at that locality (i.e., the pre-impact target). The most noticeable difference is the much higher MgO, CaO, Na_2O, K_2O, and P_2O_5 as well as the slightly lower percentages of SiO_2 and Al_2O_3 as shown in Fig. 8. Such contrast between glass and target sediments is not apparent for the RC glass/target [5].

The composition of the Pleistocene UCdM glasses differs from the older Pliocene MdP glasses previously reported [7]. Table 3 reveals that the average major element bulk glass composition from UCdM (three samples) exhibits a higher silica content (~63 wt% after correction for LOI) than the typical MdP glasses, but less than that in RC glass (~66 wt%). But the UCdM glasses contain much higher P_2O_5 percentages (typically greater than 1 wt% vs. less than 0.5 wt% for both MdP and RC), higher CaO (nearly 6 wt% for UCdM vs. 4 wt% for RC and 2 wt%

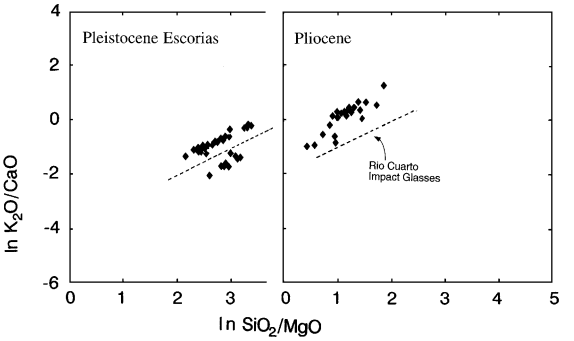

Fig. 7. Comparisons of volatile and refractory components within the clear Holocene glasses from Rio Cuarto (RC), the Pleistocene glasses from Centinela del Mar (CdM), and the mid-Pliocene from near Mar del Plata. Data are based on electron microprobe analyses of interstitial glass.

Table 3
Major element comparisons: bulk glasses and bulk loess[a]

	Glasses					Host sediments			
	RC-1E	UCdM-1E	UCdM-2E	UCdM-3E	MdP-1E	RC-Sed (L2)[b]	CdM-Sed	MdP-Sed (LCh)	MdP-Sed (L'Ant)
SiO_2	65.54	59.09	62.08	62.07	60.93	65.80	59.55	55.63	56.64
TiO_2	0.61	0.74	0.7	0.62	0.65	0.6	0.69	0.59	0.78
Al_2O_3	13.72	12.47	12.85	11.60	16.88	14.80	14.27	14.05	13.77
Fe_2O_3	4.56	5.23	4.89	4.45	7.39	4.32	5.04	4.84	4.14
MnO	0.006	0.01	0.01	0.06	0.006	0.07	0.003	0.02	0.06
MgO	2.31	3.92	3.44	3.06	2.83	1.26	1.97	2.67	1.90
CaO	4.16	6.46	4.38	5.69	2.36	3.44	2.32	2.93	3.03
Na_2O	2.83	5.38	4.28	3.77	3.41	3.49	2.58	3.89	4.32
K_2O	3.80	3.05	2.32	4.13	2.19	2.58	2.14	1.86	1.94
P_2O_5	0.49	1.18	0.75	1.31	0.14	0.15	0.2	0.19	0.56
LOI	1.22	2.37	3.27	2.97	2.78	2.90	10.38	13.83	11.93
Total	99.25	99.90	98.97	99.73	99.57	99.40	99.14	100.50	99.07

[a] XRF data in wt% by C.K., University of Vienna.
[b] 'RC Sed' refers to sample notation and values in [20].

for MdP), and higher Na_2O (almost 5 wt% for UCdM vs. 2–3 wt% at RC and ~4 wt% at MdP).

The Argentine impact glasses more strictly represent 'impact melt breccias' where the individual xenocrysts were incorporated during excavation from the crater or during dynamic emplacement. Consequently, the melt fraction may represent a source region different from that for the constituent minerals and bulk analyses would mask their provenance. Microprobe analyses of just the clear interstitial glasses for the UCdM samples reveal significant differences between their compositions, and the bulk glass for both volatile and refractory components (Tables 3 and 4 and Fig. 8). The Na_2O percentage averages about 4.6 wt% in the bulk glass (Table 3), but this value increases to as high as 8 wt% in the interstitial glasses. Similar enhancements in the interstitial glass occur for CaO (increasing from 5 to 10 wt%), P_2O_5 (from 1 to 2 wt%), and MgO (from 3.6 to 6 wt%). The K_2O, Al_2O_3, and TiO_2 contents, however, are not significantly changed.

In contrast with the UCdM glasses, the primary difference in composition between the RC interstitial glasses (clear) and the host sediment is a modest increase in K_2O, Na_2O, and CaO, consistent with minor incorporation of calcretes at depth and/or the preferential melting of feldspars [5]. The RC glasses (both the fresh and weathered) incorporated near-surface materials without significant additions of unusual substrates, based on [20].

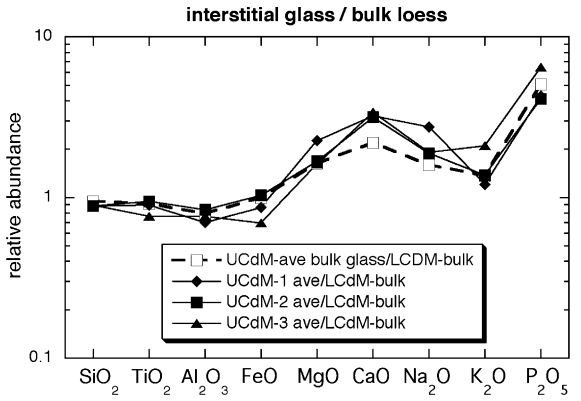

Fig. 8. Ratio of major element compositions for clear interstitial glass (electron microprobe with sodium loss routine) and bulk UCdM glass composition (XRF) to bulk loess composition (LCdM) from below (about 2 m) the impact glass layer. Significant enrichment in MgO, CaO, Na_2O, and P_2O_5 is consistent with incorporation of marine sequences (evaporites) at depth.

Table 5 provides the trace and rare earth element compositions for both the host sediment and impact glasses. While generally similar, UCdM glass compositions differ from their host sediments. There is also a systematic change in certain elements as a function of glass age. The greatest contrasts are in the relative amounts of V, Rb, Th, Sc, La_N, Yb_N, Zr, and Hf. As discussed below, the geochemical differences between the bulk glass and the pre-impact materials at each site provide clues for incorporation of materials from depth.

Table 4
Major element composition for interstitial UCdM glasses

	A(8)	B(7)	C(5)	D(9)	E(6)	F(7)
SiO_2	59.5 (1.6)	58.8 (1.5)	58.8 (0.4)	59.6 (1.9)	51.7 (1.4)	57.3 (1.9)
TiO_2	0.58 (0.08)	0.69 (0.11)	0.73 (0.16)	0.59 (0.11)	1.9 (0.2)	0.69 (0.17)
Al_2O_3	10.4 (1.4)	11.1 (0.9)	13.3 (1.7)	12.2 (3.2)	10.3 (0.8)	10.5 (2.4)
FeO	4.3 (0.7)	4.4 (0.6)	5.2 (0.4)	3.5 (0.9)	8.7 (0.5)	5.5 (0.9)
MgO	4.5 (0.5)	5.0 (0.9)	3.7 (0.7)	3.6 (1.4)	3.3 (0.4)	4.9 (0.7)
CaO	8.6 (1.3)	8.4 (0.6)	8.2 (1.4)	8.8 (2.9)	16.2 (1.5)	13.1 (2.3)
Na_2O	8.0 (0.6)	7.9 (0.8)	5.4 (0.6)	5.5 (0.7)	3.1 (0.1)	3.3 (0.6)
K_2O	2.9 (0.4)	2.9 (0.3)	3.3 (0.1)	5.0 (0.8)	3.0 (0.4)	2.2 (0.5)
P_2O_5	1.5 (0.5)	0.94 (0.16)	0.90 (0.4)	1.4 (0.7)	1.3 (0.4)	2.8 (0.5
Total	100.3 (0.5)	100.1 (0.3)	99.6 (0.3)	100.2 (0.5)	99.7 (0.8)	100.3 (0.5)

Electron microprobe analyses performed at Brown's NSF/Keck Microprobe facility with a Na loss routine described in [36]. Number of measurements for separate localities of clear class given above; standard deviation (1σ) shown in parentheses next to each value.

Table 5
Geochemistry of impact glasses from RC, CdM, and MdP

	Minor elements									
	Glasses					Host Sediments				
Sample Number	RC-1E	CdM-1E	CdM-2E	CdM-3E	MdP-1E	RC Sed(L2)*	RC-Sed (AR-5)	CdM-Sed	MdP Sed(LCh)	MdP Sed(Lant)
V	86	95	87	81	99	73.70	NA	78	90	104
Sc	10.5	11.9	11.3	10.7	12.7	5.34	9.53	12.4	12.2	13.8
Cr	34.1	34.9	31.5	29.4	34.8	35	27.8	28.5	30.7	32.5
Co	8.86	8.91	8.74	7.88	9.55	7.8	8.71	9.76	10.5	11.5
Ni	9	8	10	9	10	13.9	30	12	9	12
Cu	<2	<2	4	3	<2	26.1	NA	8	<2	9
Zn	38	49	34	18	19	64.3	75	68	52	67
Ga	12	20	10	20	15	20.9	10	5	90	17
As	3.61	2.21	1.56	4.61	5.18	NA	7.45	5.84	9.37	7.91
Se	0.3	0.9	0.8	0.2	0.5	NA	0.49	0.6	0.7	0.4
Br	0.8	6.8	0.9	5.6	8.9	NA	0.38	31	124	36
Rb	107	57.4	53.1	65.8	61.7	95.6	97.2	85.7	68.2	62.8
Sr	339	466	381	356	438	352	410	296	339	342
Y	27	25	34	26	24	17.8	NA	31	27	23
Zr	208	198	205	174	184	226	300	221	179	195
Nb	11	10	10	9	9	8.64	NA	12	11	11
Sb	0.51	0.29	0.06	0.33	0.32	NA	0.67	0.7	0.43	0.67
Cs	5.52	2.16	2.30	2.65	3.29	NA	4.43	5.22	4.45	4.01
Ba	556	456	452	431	484	612	320	403	275	364
La	28.1	21.5	24.6	23.1	21.2	22.6	27.2	22.6	21.8	18.5
Ce	54.9	46.1	44.3	40.0	46.3	50.8	48.9	54.2	45.3	42.6
Nd	26.8	24.9	25.8	22.1	22.6	23	25.4	25.8	23.5	20.1
Sm	5.65	4.44	4.68	4.93	4.29	4.16	5.12	4.29	5.08	3.70
Eu	1.11	1.13	1.33	1.08	1.18	0.64	1.08	1.15	1.13	1.06
Gd	5.3	4.4	5.5	4.2	3.9	4.76	4.7	4.7	4.4	3.2
Tb	0.79	0.74	0.93	0.74	0.71	0.6	0.85	0.75	0.77	0.56
Tm	0.47	0.43	0.47	0.39	0.36	0.28	0.37	0.43	0.42	0.34
Yb	2.81	2.82	3.09	2.65	2.49	2.05	2.33	2.66	2.55	2.33
Lu	0.41	0.41	0.48	0.42	0.37	0.321	0.35	0.41	0.37	0.34
Hf	6.31	6.82	5.91	4.75	5.48	5.96	6.89	5.76	4.89	5.27
Ta	0.79	0.68	0.56	0.52	0.59	0.79	0.76	0.59	0.56	0.48
W	1.2	0.9	0.4	1.5	0.6	1.33	0.73	0.4	0.9	0.5
Ir (ppb)	0.2	<0.5	0.2	<0.8	<0.5	NA	<10	<0.3	<1	<1
Au (ppb)	<5	6	5	3	200	NA	0.6	2	2	1
Th	11.5	8.19	7.72	7.24	7.43	8.85	10.7	9.65	7.06	6.96
U	3.11	1.21	0.98	1.43	1.75	3.35	2.54	1.28	1.54	0.94
K/U	10182	21006	19728	24068	10429		8661	13932	10065	17199
Zr/Hf	33.0	29.0	34.7	36.6	33.6		43.5	38.4	36.6	37.0
Hf/Ta	7.99	10.0	10.6	9.13	9.29		9.07	9.76	8.73	11.0
Th/U	3.70	6.77	7.88	5.06	4.25		4.21	7.54	4.58	7.40
LaN/YbN	6.76	5.15	5.38	5.89	5.75		7.89	5.74	5.78	5.37
Eu/Eu*	0.62	0.78	0.80	0.73	0.88		0.673	0.78	0.73	0.94

C. Koeberl, Univ. Vienna, January 1, 2002; *[20].
XRF and INAA data – trace elements in ppm except as noted.

4. Discussion and implications

At least four late Quaternary impacts are recorded in the Pampean sediments and were sufficient to generate significant quantities of impact glass: about 3–6 ka, 114 ka, 230 ka, and 445 ka. The radiometric dates, stratigraphic context, and composition now allow distinguishing clearly between the RC and CdM impacts. This record has several implications not only for the impact process in sedimentary targets, but also for the general stratigraphic record in an important Pleistocene exposure of the Pampean sediments.

4.1. Centinela del Mar impact

The parent craters for both CdM impacts are not presently exposed. Possible incorporation of materials from depth, however, may allow constraining estimates for the diameter of the UCdM crater. The addition of components not present in the pre-impact host sediments (below the glass layer) indicates a large event.

The major element content of Quaternary loess varies little throughout Argentina [21]. These deposits developed syngenetically with the uplift of the Andes as fluvially transported sediments from the west were redistributed during episodic and cyclic climate changes [3]. Consequently, systematic changes of minor constituents in the loess might be expected with time (and hence depth) due to changing sources for these sediments from the late Miocene into the Holocene. Average continental source materials, for example, might be supplemented by increasing contributions from younger Andean silicic volcanics over time. Although such a trend has not been previously reported, the dated impact glasses constrain the timing of emplacement and allow the exploration of this possibility. Systematic geochemical differences in different-age outcrops then might allow recognizing possible signatures of deeper (older) sediments melted or trapped in the RC, CdM, and MdP impact glasses.

Inferred changes in the source regions through time based on trace and minor elements, however, can be masked by chemical alterations on a local scale (e.g., removal or deposition of soluble components in lacustrine deposits in certain exposures). Consequently, sediment samples analyzed for the present study were selected from freshly exposed outcrops where the depositional environment (fluvial vs. eolian) could be clearly assessed. Analysis of these loose bulk loess sediments yielded a chemical index of alteration [22] value near 51, consistent with only minor alteration relative to their igneous source region. This result contrasts with previous studies that noted significant chemical alteration for Holocene and Pleistocene Argentine loess from a drill hole taken west of Buenos Aires [23]. The difference in conclusions reflects both a different environmental setting and source regions for materials at the locality used in [23].

Several key trace and rare earth element ratios can be useful for assessing subtle but meaningful compositional differences. The Th/Sc ratio, for example, can provide a sensitive index for the provenance of bulk composition [24]. The Rb/V ratio provides a similar contrast, provided that the material has not been heavily altered. Late Cenozoic silicic and mafic ash layers sampled in the loessoid deposits provide useful references for assessing possible end-member contributions that could contribute to the sediments with time or depth. The Th/Sc ratio for the volcanic ashes ranges from 4.2 (silicic) to 0.073 (mafic) and for Rb/V, from 6 (silicic) to 0.077 (mafic). These ratios represent bulk compositions and not just the volcanic (glass) component. Fig. 9A illustrates the change in bulk loess compositions for samples taken at different stratigraphic levels. It reveals that the silicic component appears to have increased with time. Although exhibiting less contrast, La_N/Yb_N and Zr/Hf ratios display the same systematic change (Fig. 9B).

The Rb/V and Th/Sc ratios for the CdM glasses are distinct from those of the host sediments (Table 5): 0.67 (glass) vs. 1.1 (host sediments) for Rb/V and 0.78 (glass) and 0.68 (host sediments) for the Th/Sc. These host sediments are estimated to be about 0.23 Ma based on their location near the same level as the dated LCdM glasses (230 ka). Because the Rb/V ratio provides the greatest contrast between mafic and silicic compositional extremes, it is used here as a preliminary index to

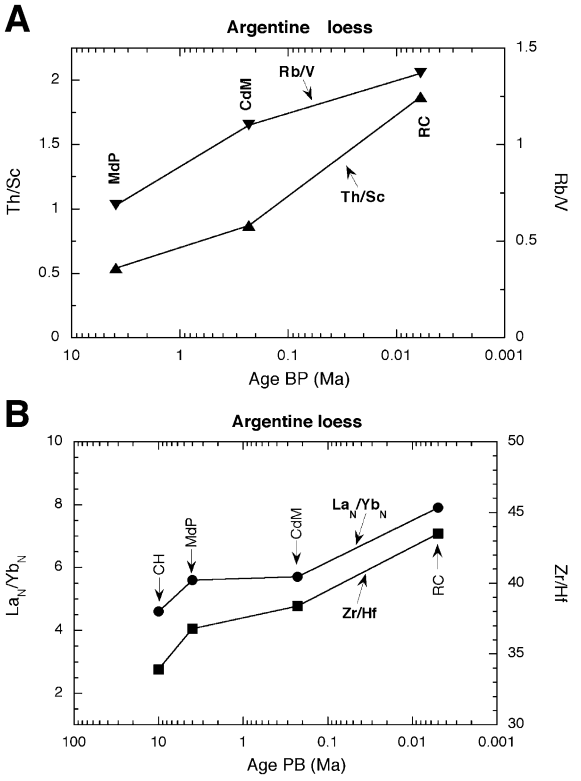

Fig. 9. Comparison of selected minor, trace and rare earth elements within bulk loess samples suggesting systematic change in sediments through time. RC represents averaged values for the upper 1.5 m of loess at Rio Cuarto. CdM indicates value for bulk loess below the glass horizon (pre-impact) at Centinela. MdP represents Pliocene (Lower Chapadmalal) and CH, Miocene Chasicoan materials. Panel A shows changes in Th/Sc and Rb/V while Panel B shows changes in La_N/Yb_N and Zr/Hf. The change in these ratios is consistent with an increasing contribution of silicic components through time. End-member compositions can be represented by Late Cenozoic mafic and silicic ash layers sampled in the loessic sections at different localities (see text).

assess the possible incorporation of older (deeper) loess sequences components captured in the impact glass (Fig. 10). If the Rb/V values trapped in the glass primarily represent the provenance of the loess component, then Fig. 10 indicates that the UCdM glasses incorporated materials with values comparable to sediments with an average age of nearly 4 Ma, based on stratigraphy and the dated MdP impact glasses [7]. This composition might correspond to a depth of about 50–100 m below the pre-impact surface at Centinela. In contrast, the difference between the bulk RC glass and the near-surface pre-impact sediments is negligible, consistent with conclusions of earlier studies [5,20]. Future studies assessing the platinum group elements or isotopic composition of highly siderophile elements (e.g., [25]) should provide a clearer picture of the inferred evolution of the source regions, and hence the excavation depths.

The stratigraphic section in the CdM region is poorly constrained and relies on seismic studies, rather than direct sampling. Previously acquired reflection seismic profiles paralleled (southwest to northeast) the coastline for a distance of 16–20 km between Necochea and Mar del Sur and crossed near the Centinela site. The seismic basement was found at depth and ranged from 430 m (near Necochea) to around 453 m (5 km away southwest from Centinela) and finally to 477–380 m at Mar del Sur [26]. One interpretation by Schillizi [26] suggested that the seismic basement correlated with the Paleozoic sandstones, which occur at a depth of 291 m in Necochea [27].

A more recent regional reconstruction by Frylund et al. [28], however, suggests that the seismic basement proposed in [26] instead corresponds to the Tandilia system, which represents a Precambrian metamorphic and igneous shield covered by

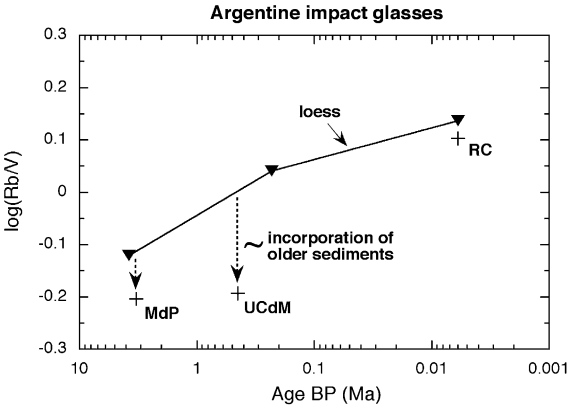

Fig. 10. Comparison of Rb/V ratio for bulk loess and impact glasses from different localities. At RC, impact glass and near-surface loess exhibit very similar values consistent with previous conclusions [19]. The average of three CdM glasses, however, has a value suggesting incorporation of much older (deeper) sediments, thereby indicating a large impact. The MdP glasses [7] also appear to have incorporated deeper sediments.

early Paleozoic sediments. In this interpretation, the Paleozoic cover sediments divide into three main intervals based on the seismic velocities. The lowermost interval is attributed to the upper Miocene (37–73 m thick) at a depth of 300–450 m. The middle interval (328–365 m thick) correlates with Pliocene loessoid sediments, the top of which is barely exposed at CdM. And the uppermost interval is attributed to the Quaternary with a thickness ranging from 28 to 44 m [26]. This latter interval is poorly represented in the coastal section at CdM but characterizes surface sediments farther inland. Consequently, in this interpretation the entire cover in this region represents sedimentary sequences extending to a depth of 400–500 m.

The CdM area is located northward of the northern margin of the Colorado sedimentary basin, which contains thick marine deposits (including evaporites) of Tertiary age. Moreover, the Pedro Luro Formation (a Paleocene marine unit) is located 40–60 km offshore from the CdM outcrop [28]. Consequently, the extensive Miocene marine transgression that inundated most of the Argentinean sedimentary basin is very likely recorded at depth as well and would cover the margins of the Pampa interserrana area, as indicated in a paleogeographic map by Ramos [29]. Such Tertiary marine evaporites at the base of the Paleozoic sediment cover could account for the elevated CaO, MgO, and P_2O_5 contents measured in the glass (see Fig. 8), as well as the direct correlation between the CaO and P_2O_5 abundances. It is also reinforced by the higher Sr values (401 ppm, average of three) and K/U (21 600) relative to the local loessoid material slightly lower in the section (222 ppm and 10 269, respectively).

These two approaches (sediments from depth and possible marine components) allow constraining the size of the primary impact crater responsible for the UCdM glasses. It is possible that some of the larger (>100 μm), rounded quartz grains entrained in the glasses may have been derived from Paleozoic quartzites, but more detailed studies will be required to confirm such a possibility. Nevertheless, the impact glasses do contain compositional evidence for materials at depth including a component that could correspond to marine transgressions within the upper Miocene sequences at a depth of 328–365 m [28]. Consequently, the maximum transient excavation depth (half of the transient crater depth) probably did not exceed 400–500 m. As a result, the transient crater diameter may have been as large as 4 km collapsing to form a complex impact structure exceeding 6 km in diameter soon after formation (or more likely a multi-ring structure due to the soft sediments).

4.2. Rio Cuarto impacts

At least two different events are now represented in the loess sequences near Rio Cuarto. The older component, dated here at 114 ka, however, is significantly different from the value of 570 ± 100 ka reported in [6]. That study proposed a possible connection with our 445 ka UCdM coastal site, which is nearly 800 km to the east. The high glass content and composition of the UCdM glasses, however, seem inconsistent with the clast-rich materials typically found at Rio Cuarto.

The extensive collection of impact glasses recovered from Rio Cuarto cannot be collectively called ‘tektites’ as suggested in [6]. Tektites refer to a very specific type of high-temperature impact glass product without microcrystites, xenocrysts, and extensive vesiculation [30–32]. Moreover, they generally have very low contents of water and volatile alkalis (K and Na), in contrast with most of the Argentine glasses. Previously published descriptions of these glasses [4,5,20] noted the wide range of glass types present, with clast content ranging from 10 to more than 80 vol%. The generation of impact glass requires sufficiently large objects to survive atmospheric entry with sufficiently high velocities to melt soils to very high temperatures. For example, the Campo del Cielo meteorites produced a field of 10–50-m-sized craters and deeply buried meteorites strewn across the Chaco plain [33,34]. The largest structures appeared to be ‘explosion’ craters without preserved meteoritic material associated with them. But this widespread event failed to generate any glass, either within the structures or as ejecta [33]. Analysis of a few fused materials initially

reported at that site subsequently proved to be ceramics of human origin. In general, most impact craters or crater fields with sizes smaller than 0.5 km in diameter fail to generate significant glass. The Rio Cuarto event, however, was sufficiently large to generate and disperse material recovered over a corridor extending at least 150 km to the southwest.

The Rio Cuarto impact glasses may have been produced by a large oblique impact [4,5] or perhaps by widespread melting of soils following catastrophic failure during entry [6]. Both scenarios would account for the evidence for shallow excavation and glass dispersal. The radiometric and fission track ages (3–6 ka) for fresh-appearing glasses at Rio Cuarto, however, are consistent with the radiocarbon exposure ages ($\sim$4 ka) for carbon within floor sediments from one of the large elongate structures (cited in [6]). The age of the younger glasses is also consistent with the preservation state of partially melted meteorites recovered from the structures [5]. The younger event either excavated the older glasses from depth, or they were subsequently exposed through later eolian deflation, which is recognized as an ongoing process within the structures [5].

Consequently, the hypothesis of a recent oblique impact for the RC materials (and some of these structures) not only remains viable, but is also consistent with data in hand: 3–6 ka impact glasses; 4 ka sediment carbon dating from the floor of one of the structures; preservation state of associated meteorites; shallow excavation; widespread dispersal of impact glasses within a corridor extending at least 150 km long; and high-temperature products recovered farther to the southwest. Systematic field studies now under way will fully explore this historic event and the source crater for older glasses in the same region.

5. Conclusions

Late Cenozoic impact glasses ('pampasites') captured in the loessoid deposits of Argentina are providing invaluable insights into the terrestrial impact record similar to the role of Antarctica for preserving meteorites. They also allow revision of the stratigraphic record by establishing critical benchmarks for magnetostratigraphy and biostratigraphy. The major conclusions from the current inventory of Late Quaternary impacts from Rio Cuarto and Centinela del Mar include the following.

1. The well-dated glasses from Centinela del Mar of 445 ± 21 ka (UCdM) and 230 ± 40 (LCdM) establish exposures of two new impact deposits preserved in the Argentine loess.
2. Systematic changes in the geochemistry of both sediments and impact glass since at least the early Pliocene appear to correspond to increasing contributions from Andean silicic sources through time.
3. The Centinela (UCdM) impact glasses appear to have incorporated not only deeper loessoid sediments (based on the interpreted compositional evolution of the loess) but also a marine evaporite component (enhanced levels of MgO, CaO, Na_2O, K_2O, and P_2O_5). This observation suggests a final crater size as large as 6 km that is now buried or is offshore.
4. At least two separate impact events can be recognized at Rio Cuarto with clearly distinguished dates of 3–6 ka and 114 ka (both from multiple samples) and are distinct in both age and chemistry from widespread glasses recovered at CdM.
5. The radiometric and fission track ages for the fresh-appearing RC impact glasses from this study are consistent with both their preservation state and AMS carbon-dated sediments within one of the elongate structures [6].
6. Most impact glasses at RC represent impact melt breccias and do not meet the established criteria for tektites.
7. The significance of a date of ca. 570 ± 100 ka (reported in [6]) for a single glass fragment recovered at RC is unclear. This date may reflect disturbed materials (with alteration and/or extraneous argon) that were derived from either the ca. 6 ka or 114 ka events. Although it conceivably could represent distal materials from the 445 ka UCdM impact [6], such materials should be rare at RC. Lastly, it could reflect still another impact, which would still be consistent with the expected impact flux.

8. The Rio Cuarto impacts incorporated materials from near the surface, consistent with shallow excavation by an oblique impact (or near-surface break-up).
9. Glass occurrences recovered from the Pampean sediments of Argentina should not be arbitrarily linked to specific events without first establishing age, stratigraphic setting, and geochemistry due to the rich and well-preserved impact record.

Separate contributions will examine the nature and occurrence of the older Miocene (5.2 and 9.2 Ma) impact glasses recovered in other localities [9], the paleomagnetic record [35], and the implications for the stratigraphy at Centinela as well as the loess stratigraphy of Argentina in general. Additional Late Cenozoic impact materials should be expected, particularly if impact craters as small as 0.5 km can yield significant glassy products from this unique depositional setting.

Acknowledgements

The authors gratefully acknowledge the thorough reviews by Bill Glass and Scott McLennan. This research was supported by grants (P.H.S., W.H., T.E.B., P.R.) from the National Science Foundation (EAR-0001047) and from CONICET (M.A.Z.). Electron microprobe analyses were performed at both the NSF/Keck Facility at Brown University (P.H.S.) with the assistance of Joe Devine and the microprobe facility at Northern Arizona State University (T.B. and J.W.). C.K. is supported by the Austrian Science Foundation, Project Y58-GEO.*[KF]*

References

[1] R.A.F. Grieve, A.M. Therriault, L.K. Kreis, Impact structures of the western sedimentary basin of North America: New discoveries and hydrocarbon resources, in: J.E. Christopher et al. (Eds.), Eighth International Williston Basin Symposium, Saskatchewan Geol. Soc. Spec. Publ. 13 (1998) 189–201.

[2] A. Montanari, C. Koeberl, Impact Stratigraphy, Springer-Verlag, New York, 2000, 364 pp.

[3] M.A. Zárate, Loess of southern South America, Quat. Sci. Rev. 22 (2003) 1987–2006.

[4] P.H. Schultz, R.E. Lianza, Recent grazing impacts on the Earth recorded in the Rio Cuarto crater field, Argentina, Nature 355 (1992) 234–237.

[5] P.H. Schultz, C. Koeberl, T.E. Bunch, J.A. Grant, W. Collins, Ground truth for oblique impact processes: New insight from the Rio Cuarto, Argentina, crater field, Geology 22 (1994) 889–892.

[6] P.A. Bland, C.R. deSouza Filho, A.J.T. Tull, S.P. Kelley, R.M. Hough, N.A. Artemieva, E. Pierazzo, J. Coniglio, L. Pinotti, V. Evers, A.T. Kearsley, A possible tektite strewnfield in the Argentine pampas, Science 296 (2002) 1109–1111.

[7] P.H. Schultz, M.A. Zárate, W. Hames, C. Camilion, J. King, A 3.3 Ma impact in Argentina and possible consequences, Science 282 (1998) 2061–2063.

[8] P.H. Schultz, M.A. Zárate, W. Hames, Three new Argentine impact sites: Implications for Mars, Lunar Planet. Sci. Conf. XXX (1999) Abstract 1898, CD-ROM.

[9] P.H. Schultz, M.A. Zárate, W. Hames, J. King, C. Heil, C. Koeberl, P.R. Renne, A. Blasi, Argentine impact record, Geol. Soc. Am. Abstr. Progr. 34 (2002) 401.

[10] P.H. Schultz, M.A. Zárate, J. King, A. Blasi, W. Hames, Formation and evolution of impact craters in the Argentine Pampas, Actas del XV Congreso Geologico Argentino, 2002, pp. 179–181.

[11] E.M. Shoemaker, R.F. Wolfe, C.S. Shoemaker, Asteroids and comet flux in the neighborhood of Earth, Geol. Soc. Am. Spec. Pap. 247 (1990) 155–170.

[12] F.I. Isla, N.W. Rutter, J.E. Schnack, M.A. Zárate, La transgresión belgranese en Buenos Aires. Una revisión a cien anõs de su definición, Cuat. Ci. Ambient. 1 (2000) 3–14.

[13] C. Frondel, Dana's The System of Mineralogy: Vol. III, Silica Minerals, John Wiley and Sons, New York, 1962, 334 pp.

[14] W.A. Deer, R.A. Howie, J. Zussman, Rock-forming Minerals: Vol.e 4, Framework Silicates, John Wiley and Sons, New York, 1963, 435 pp.

[15] P.R. Renne, W.D. Sharp, A.L. Deino, G. Orsi, L. Civetta, $^{40}Ar/^{39}Ar$ dating into the historical realm: Calibration against Pliny the younger, Science 277 (1997) 1297–1298.

[16] P.R. Renne, C.C. Swisher, A.L. Deino, D.B. Karner, T. Owens, D.J. DePaolo, Intercalibration of standards, absolute ages and uncertainties in $^{40}Ar/^{39}Ar$ dating, Chem. Geol. (Isot. Geosci. Sect.) 145 (1998) 117–152.

[17] D. Storzer, Fission track dating of some impact craters in the age-range between 6000 y and 300 my, Meteoritics 6 (1971) 319.

[18] D. Storzer, E.K. Jessberger, J. Kunz, J.M. Lange, Synopsis von Spalspuren und Kalium-Argon Datierungen an Rise-Impaktgläsern und Moldaviten, Exk. Veröff. GGW Berlin 195 (1995) 79–80.

[19] D. Storzer, G.A. Wagner, The application of fission track dating in stratigraphy: a critical review, in: G.S. Odin

(Ed.), Numerical Dating in Stratigraphy, Wiley and Sons, Chichester, 1982, pp. 199–221.
[20] A.A. Aldahan, C. Koeberl, G. Possnert, P.H. Schultz, ^{10}Be and chemistry of impactites and target materials from the Rio Cuarto crater field, Argentina: Evidence for surficial cratering and melting, Geol. Forsch. Fortschr. 119 (1997) 67–72.
[21] M.E. Teruggi, The nature and origin of Argentina loess, J. Sediment. Petrol. 27 (1957) 322–332.
[22] S.R. Taylor, S.M. McLennan, The Continental Crust: Its Composition and Evolution, Blackwell, Oxford, 1985, 312 pp.
[23] S. Gallet, B. Jah, B.V.V.L. Lanoe, A. Dia, E. Rosell, Loess geochemistry and its implications for particle origin and composition of the upper continental crust, Earth Planet. Sci. Lett. 156 (1998) 157–172.
[24] S.M. McLennan, S. Hemming, D.K. McDaniel, G.N. Hanson, Geochemical approaches to sedimentation, provenance and tectonics, in: Processes Controlling the Composition of Clastic Sediments, Geol. Soc. Am. Spec. Pap. 284 (1993) 21–40.
[25] B. Peucker-Ehrenbring, B. Jahn, Rhenium-osmium isotope systematics and plantinum group element concentrations: Loess and the upper continental crust, Geochem. Geophys. Geosyst. 2 (2001) (2001GC000172).
[26] R. Schillizzi, Reconocimiento sismico del litoral sur marplatense, provincia de Buenos Aires, Rev. Asoc. Geol. Argentina XLI (1986) 182–186.
[27] L. Lambias, E.J. Prozzi, C.R. Prozzi, Ventania, in: Relatorio Geologia de la Provincia de Buenos Aires, VI Congreso Geológico Argentino, Bahia Blanca, 1975.
[28] B. Frylund, A. Marshall, J. Stevens, Geologia y Recursos Naturales de la Plataforma Continental Argentina, Cuenca del Colorado en XIII Congreso Geologico Argentina y III Congreso de Exploracion de Hidrocarburos, Buenos Aires, vol. 8, 1996, pp. 135–158.
[29] V.A. Ramos, Los depósitos sinorogénicos terciaros de la región andina, Geol. Argentina Inst. Geol. Recur. Miner. Anales 29 (1999) 651–682.
[30] B.P. Glass, M.B. Swincki, P.A. Zwart, Australasian, Ivory Coast and North American tektite strewnfields: Size, mass and correlation with geomagnetic reversals and other earth events, Proc. Lunar Planet. Sci. Conf. 10 (1979) 2535–2545.
[31] C. Koeberl, Geochemistry of tektites and impact glasses, Annu. Rev. Earth Planet. Sci. 14 (1987) 323–350.
[32] C. Koeberl, Tektite origin by hypervelocity asteroidal or cometary impact: Target rocks, source craters, and mechanisms, in: B.O. Dressler, R.A.F. Grieve, V.L. Sharpton (Eds.), Large Meteorite Impacts and Planetary Evolution, GSA Spec. Pap. 293 (1994) 133–152.
[33] W.A. Cassidy, L.M. Villar, T.E. Bunch, T.P. Kohman, D.J. Milton, Meteorites and craters of Campo del Cielo, Argentina, Science 149 (1965) 1055–1064.
[34] W.A. Cassidy, S.P. Wright, Small impact craters in Argentine loess: A step up from modeling experiments, LPI Contrib. 1155 (2003) 14.
[35] C. Heil, J. King, M.A. Zárate, P.H. Schultz, Paleomagnetic and environmental magnetic studies of Pampeano Loess Deposits from Centinela del Mar, Argentina, EOS Trans. AGU Suppl. 83 (Fall Meet. Suppl.) (2002) GP71A-0974.
[36] J.D. Devine, J.E. Gardner, H.P. Brack, G.D. Layne, M.J. Rutherford, Comparison of microanalytical methods for the estimation of H_2O contents of silicic volcanic glasses, Am. Mineral. 80 (1995) 319–328.